

Supporting Information (SI)

**Construction of heterocycle-triazolotriazine framework energetic compounds: Towards novel high-performance explosives**

Pengju Yang<sup>a,b</sup>, Xiaoxiao Zheng<sup>c</sup>, Guojie Zhang<sup>d</sup>, Caijing Lei<sup>a</sup>, Guangbin Cheng<sup>a,\*</sup> and Hongwei Yang<sup>a,\*</sup>

<sup>a</sup> *School of Chemistry and Chemical Engineering, Nanjing University of Science and Technology, Nanjing, Jiangsu, China;*

<sup>b</sup> *Tianyuan (Hangzhou) New material Technology Co., LTD, Hangzhou, Zhejiang, China;*

<sup>c</sup> *Zhejiang Dayang Biotechnology Group Co., LTD, Hangzhou, Zhejiang, China;*

<sup>d</sup> *School of materials and chemistry, Southwest University of Science and Technology, Mianyang, Sichuan, China.*

*\* Corresponding author.*

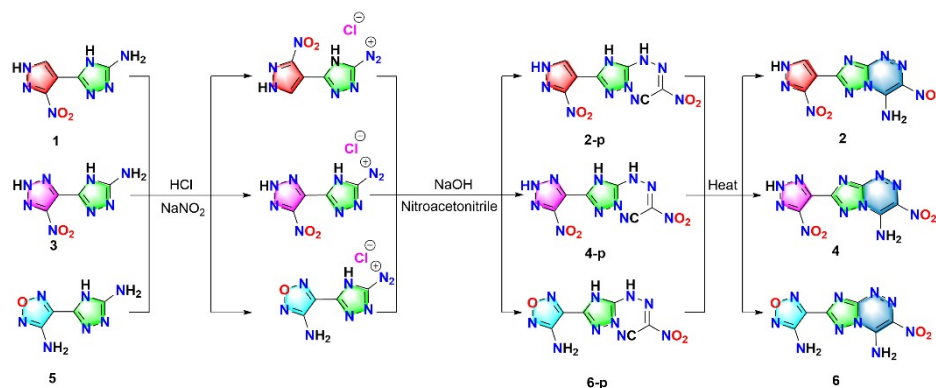
*Email: gcheng@mail.njust.edu.cn (G. Cheng); hyang@mail.njust.edu.cn (H. Yang)*

*Fax: (+) 86 25 8430 3286A*

## Table of Contents

1. Synthesis.....	1
2. TG and DSC curves.....	2
3. Theoretical calculation.....	3
4. General methods.....	5
5. Computational Details .....	5
6. Crystallographic Data for 2, 4 and 6.....	9
7. Spectrums of Compounds 2, 4 and 6.....	12
8. References.....	17

## 1. Synthesis



Scheme S1. Synthetic routes of **2**, **4** and **6**.

### **Synthesis of 3-nitro-7-(3-nitro-1H-pyrazol-4-yl)-[1,2,4] triazolo [5,1-c][1,2,4]triazin-4-amine (2)**

Substrate **1** (0.490 g, 2.5 mmol) was added to a mixture of 7.5 mL water and 1.2 mL 37% HCl. After cooling down to -5 °C, sodium nitrite (0.2 g, 2.9 mmol) dissolved in 2.5 mL H<sub>2</sub>O was dripped slowly into this mixed reaction. The resultant solution was held at 0 °C for 0.5 h during which time lots of bubbles appeared and the solid was gradually dissolved in solution. Then, the freshly prepared nitroacetonitrile sodium salt (4.0 mmol nitroacetonitrile was dissolved in the solution of 4.0 mmol NaOH in 0.5 mL H<sub>2</sub>O) was added drop by drop to this solution under 0 °C. After stirring at 0 °C for 1 h, the reaction system was warmed up to 25 °C. After 8 h, the solid was collected by filtration, washed with iced water and then dried in air to obtain a luminous yellow solid **2-p** (0.25 g, 76.0%). The yellow solid was suspended in a mixture of 10.0 mL H<sub>2</sub>O and 10.0 mL MeOH. The reaction system was refluxed for 8 h and the color darkened. The solid was collected by filtration, washed with a little cold water and further dried in air to obtain **2** as a light brown solid (0.24 g, 68.0%). <sup>1</sup>H NMR (500 MHz, DMSO-*d*<sub>6</sub>): δ = 14.43, 10.20, 9.70, 8.64 ppm. <sup>13</sup>C NMR (126 MHz, DMSO-*d*<sub>6</sub>): δ = 158.9, 156.4, 153.4, 139.4, 138.1, 134.1, 106.1 ppm. IR (KBr pellet): 3682.5, 3678.4, 3543.1, 1673.5, 1632.5, 1583.3, 1513.6, 1415.2, 1402.9, 1349.6, 1300.4, 1234.8, 1107.7, 857.6, 423.0 cm<sup>-1</sup>. Elemental analysis calcd (%) for C<sub>7</sub>H<sub>4</sub>N<sub>10</sub>O<sub>4</sub>(292.04): C, 28.78; H, 1.38; N, 47.94; O, 21.90 found: C, 28.65; H, 1.68; N, 47.69; O, 21.90.

### **Synthesis of 3-nitro-7-(5-nitro-2H-1,2,3-triazol-4-yl)-[1,2,4] triazolo [5,1-c][1,2,4]triazin-4-amine (4)**

Substrate **3** (0.490 g, 2.5 mmol) was added to a mixture of 7.5 mL water and 1.2 mL 37% HCl. After cooling down to -5 °C, sodium nitrite (0.2 g, 2.9 mmol) dissolved in 2.5 mL H<sub>2</sub>O was dripped slowly into this mixed reaction. The resultant solution was held at 0 °C for 0.5 h during which time lots of bubbles appeared and the solid was gradually dissolved in solution. Then, the freshly prepared nitroacetonitrile sodium salt (5.0 mmol nitroacetonitrile was dissolved in the solution of 5.0 mmol NaOH in 0.6 mL H<sub>2</sub>O) was added drop by drop to this solution under 0 °C. After stirring at 0 °C for 1 h, the reaction system was warmed up to 25 °C. After 8 h, the solid was collected by filtration, washed with iced water and then dried in air to obtain a luminous yellow solid **4-p** (0.23 g, 70.0%). The yellow solid was suspended in a mixture of 12.5 mL H<sub>2</sub>O and 12.5 mL MeOH. The reaction system was refluxed for 8 h and the color darkened. The solid was collected by filtration,

washed with a little cold water and further dried in air to obtain **4** as a light brown solid (0.373 g, 76.0%).  $^1\text{H}$  NMR (DMSO- $d_6$ ):  $\delta$  = 14.26, 10.50 9.80 ppm.  $^{13}\text{C}$  NMR (DMSO- $d_6$ ):  $\delta$  = 158.07, 155.39, 151.42, 137.10, 134.92, 113.83 ppm. IR (KBr pellet): 3670.7, 3633.7, 3537.5, 1665.3, 1602.4, 1583.9, 1513.6, 1410.0, 1343.4, 1299.0, 1232.4, 1125.1, 847.6, 725.5, 444.3  $\text{cm}^{-1}$ . Elemental analysis calcd (%) for  $\text{C}_6\text{H}_3\text{N}_{11}\text{O}_4$ (264.05): C, 24.58; H, 1.03; N, 52.56; O, 21.83 found: C, 24.23; H, 1.07; N, 52.45; O, 22.32.

**Synthesis of 4-(4-amino-3-nitro-[1,2,4] triazolo [5,1-c][1,2,4]triazin-7-yl)-1,2,5-oxadiazol-3-amine (6)**

The substrate **5** (0.334 g, 2.0 mmol) was fed at a time to a mixed solution of 6 mL  $\text{H}_2\text{O}$  and 1 mL 37% HCl. After cooling down to  $-5\text{ }^\circ\text{C}$ ,  $\text{NaNO}_2$  (0.160 g, 2.32 mmol) dissolved in 2 mL  $\text{H}_2\text{O}$  was added slowly to this reaction. The resultant solution was held at  $0\text{ }^\circ\text{C}$  for 0.5 h during which time lots of bubbles appeared and the solid was dissolved in the solution. Then, the freshly prepared nitroacetonitrile sodium salt (4.0 mmol nitroacetonitrile added to the mixture of 4 mmol NaOH and 0.5 mL water) was added in small batches to this solution while keeping the reaction temperature no more than  $0\text{ }^\circ\text{C}$  for 1 h. And then it was warmed up to indoor temperature. After 8 h, the solid was collected by filtration, then washed with ice water and further dried in air to obtain a light yellow solid **6-p** (0.184 g, 70.0%). The light-yellow solid was suspended in a mixed solution of 10 mL  $\text{H}_2\text{O}$  and 10 mL MeOH. The reaction mixture was refluxed overnight during which time the color of the solution darkened. The solid was collected by filtration, washed with iced water, and further dried in air to give **6** as a brown solid (0.282 g, 77.0%).  $^1\text{H}$  NMR (DMSO- $d_6$ ):  $\delta$  = 9.98, 9.21 7.09 ppm.  $^{13}\text{C}$  NMR (DMSO- $d_6$ ):  $\delta$  = 156.30, 156.00, 155.69, 139.54, 138.71, 138.24 ppm. IR (KBr pellet): 3685.5, 3585.6, 3533.8, 1661.6, 1617.2, 1572.8, 1502.5, 1358.2, 1295.3, 1232.4, 1184.3, 1054.8, 851.3, 485.0  $\text{cm}^{-1}$ . Elemental analysis calcd (%) for  $\text{C}_6\text{H}_4\text{N}_{10}\text{O}_3$  (264.05): C, 27.28; H, 1.53; N, 53.02; O, 18.17 found: C, 27.23; H, 1.47; N, 53.15; O, 18.06.

**2. TG and DCS curves**

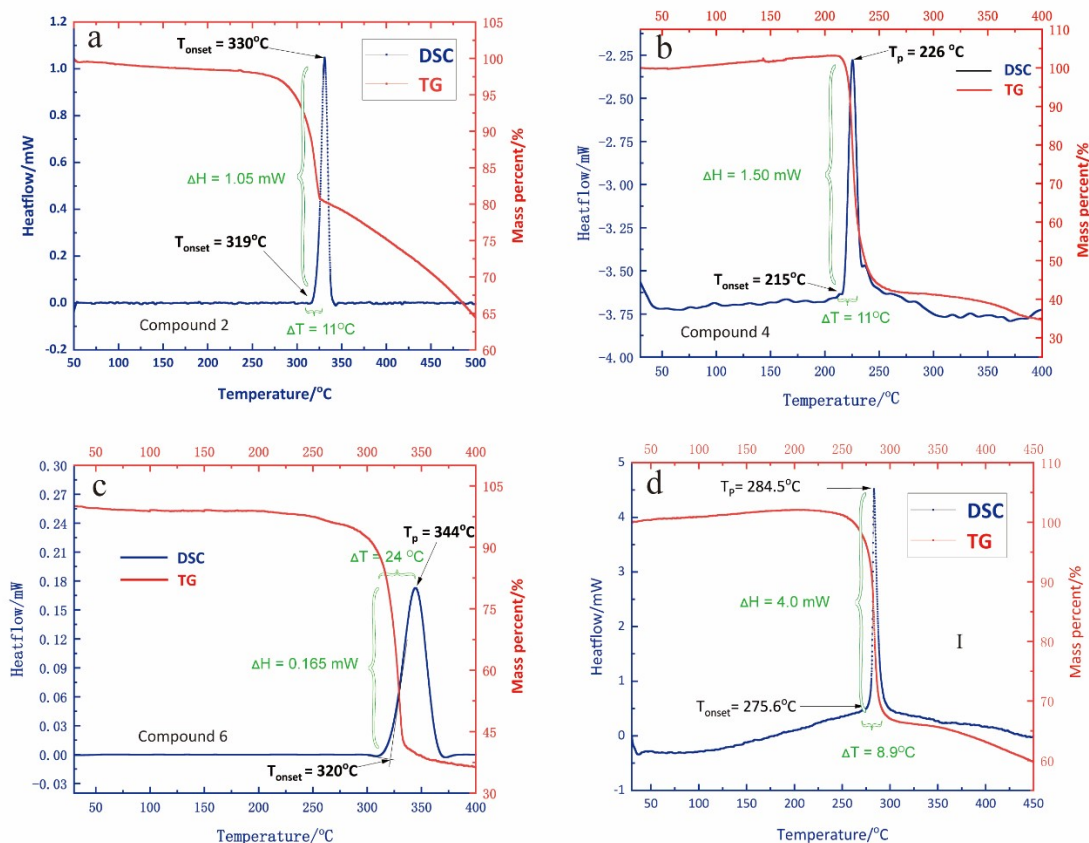


**Figure S1** TG and DSC curves for **2**, **4**, and **6**.

The thermal stability of compounds **2**, **4**, **6** and **I** was evaluated by a simultaneous thermal analyzer (DSC-TG) in a 40 mg Al-standard pan with a scanning warming rate of 10 °C min<sup>-1</sup> in a N<sub>2</sub> atmosphere. Significantly, a water bath oven was used to dry the samples at 40 °C before the test. According to the results, all these samples have no crystallized water or methanol which could be evidenced by the solvent-free DSC-TG plots in Figure S1a-S1d. Compounds **2** and **6** show high thermal stabilities and begin to decompose at 319 °C and 320 °C, and reach the maximum heat release rate at 330 °C and 344 °C, respectively. While compound **4** begins to decompose at 215 °C and reaches the maximum heat release rate at 226 °C. The heat flow changes ( $\Delta H$ ) from  $T_{\text{onset}}$  to  $T_p$  for compounds **2**, **4** and **6** are 1.05 mW, 1.50 mW and 0.165 mW, respectively. It is clear that compound **2** and **4** reaches the maximum heat release rate faster than compound **6** ( $\Delta T = 11^\circ\text{C}$ ; 24 °C), indicating their faster decomposition and potential applications as a high-energy explosive. While compound **6** with a stable energy output could be used as a heat-resistant explosive.

### 3. Theoretical calculation

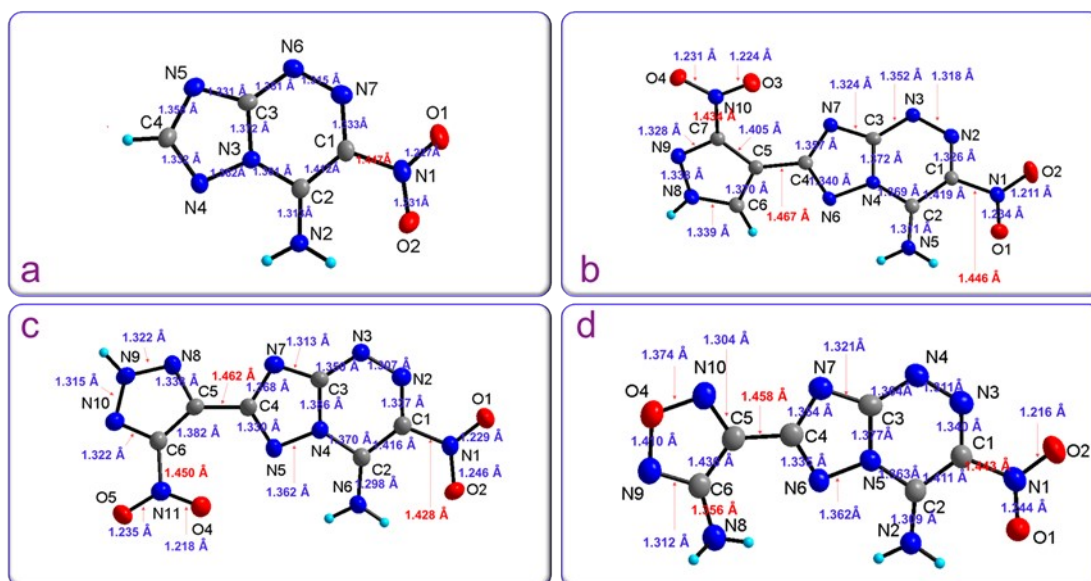


**Figure S2.** Bond lengths of **II(a)**, compound **2(b)**, **4(c)** and **6(d)**.

According to the results, the decomposition temperature of **2**, **4** and **6** are obviously different from that of **I** despite they have the same triazolotriazine structure. Bond length which is closely related to bond dissociation energy and the thermal stability of structurally similar compounds was listed in Figure S2 to analyze the influence of nitro-pyrazole, nitro-1,2,3-triazole and amino-1,2,5-oxadiazole on the thermal stability. Among the same kind of bonds, the longer the bond length, the weaker the bond dissociation energy, and the lower the thermal stability. As shown in Figure S2a-S2d, with the introduction of substituents, the length of the weakest bond (C1-N1) on **II** shortens from 1.447 Å to 1.446 Å, 1.428 Å and 1.443 Å, indicating the positive effect of the introduced substituents on the thermal stability. However, the bond lengths show quite difference nearby the nitro pyrazole, nitro-1,2,3-triazole and amino-1,2,5-oxadiazole. Due to the electron absorption of nitrogen atoms, the electrons in the pyrazole distribute more evenly than that in the 1,2,3-triazole, and the bonds which connect the nitro group with the backbone extend from 1.434 Å to 1.450 Å. This result indicates the introduction of nitro-1,2,3-triazole will weaken the bond dissociation energy significantly, leading to the lower thermal decomposition temperature of compound **4** than compound **2**. It is a good choice to insert the oxygen into the backbone to distribute the bond lengths more evenly. As shown in Figure S2d, the bond lengths are even in amino-1,2,5-oxadiazole, indicating strong conjugation which is in consistent with the high thermal stability of compound **6**.

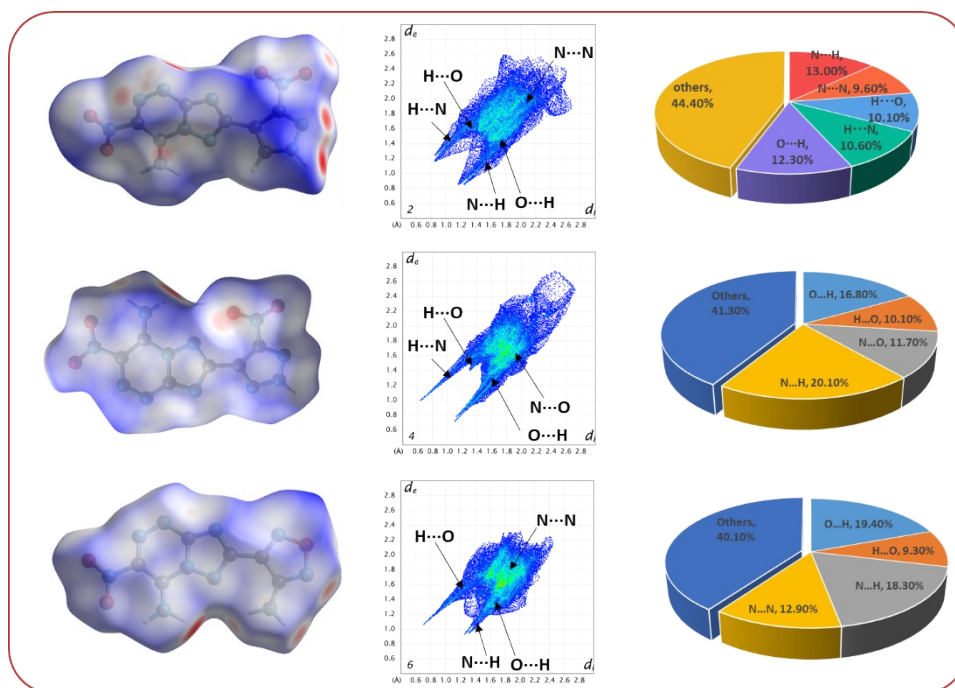


**Figure S3.** The hirshfeld surface analysis plots for compounds **2**, **4**, and **6**.

As shown in Figure S3, the two-dimensional (2D) fingerprint plots and the associated Hirshfeld surfaces based on the crystal structure of **2**, **4** and **6** were generated by using CrystalExplorer to analyze and quantify the close contact interaction and hydrogen bonds. The overall intermolecular interaction was visualized and associated with specific atoms, and the concrete percentages were recorded in the histogram. The widespread red dots indicate strong intermolecular interactions among which most are the hydrogen bonds while the blue flat areas mainly imply  $\pi$ -stacking. The interaction weakens gradually from the red dots to the blue regions. Most of the red dots in compounds **2**, **4** and **6** are distributed at the edge of the Hirshfeld surfaces. The percentage of hydrogen bond interactions in **2**, **4** and **6** is more than 40%, indicating that a large number of hydrogen bonds in both compounds and endowing **2**, **4** and **6** with relatively low mechanical sensitivities and high densities.

#### 4. General methods

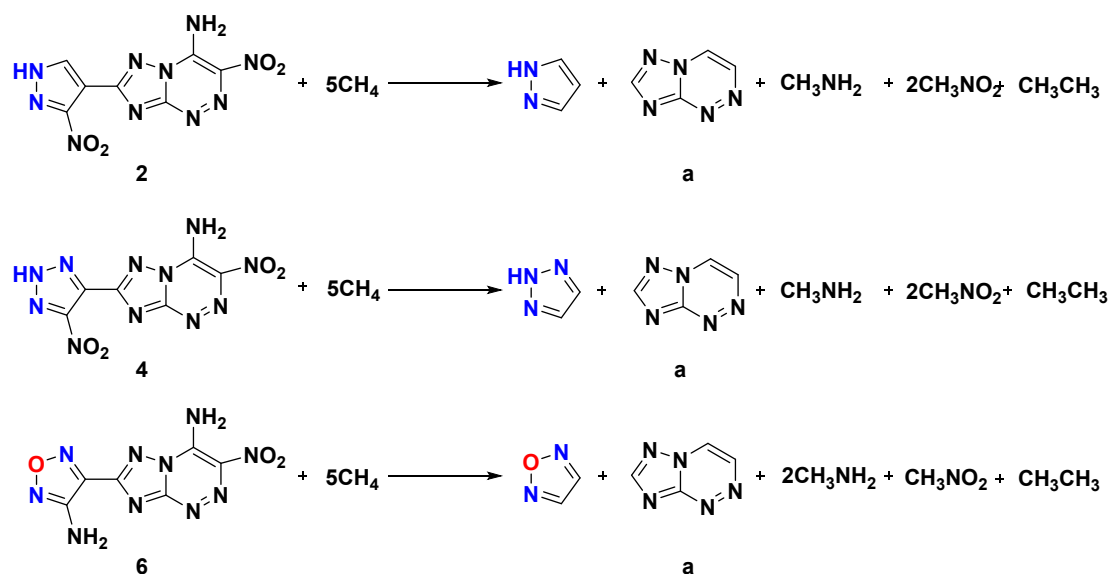
The percentages of C, H, N, and O were tested on an elemental analyser (ThermoFisher, FlashSmart). Urea was used as the standard substances.  $^1\text{H}$  and  $^{13}\text{C}$  NMR spectra were obtained by using a 500 MHz nuclear magnetic resonance spectrometer (Bruker AVANCE 500; 500 MHz for  $^{13}\text{C}$ ; 126 MHz for  $^1\text{H}$ ). DMSO- $d_6$  was used as the solvent and locking solvent. DSC was performed on an STD-Q600 instrument. Infrared (IR) spectra were recorded on a Perkin-Elmer Spectrum BX FT-IR equipped with an ATR unit. Friction sensitivity and impact sensitivity of samples are measured using the standard BAM methods.

#### 5. Computational Details

Computations were performed by using the Gaussian09 suite of programs [1]. The elementary geometric optimization and the frequency analysis were performed at the level of the Becke three parameter, Lee-Yan-Parr (B3LYP) functional with the 6-311+G\*\* basis set [2-4]. All the optimized structures were characterized to be local energy minima on the potential surface

without any imaginary frequencies. Atomization energies were calculated by the CBS-4M [5]. All the optimized structures were characterized to be true local energy minima on the potential-energy surface without imaginary frequencies.

The predictions of heats of formation (HOF) of compounds used the hybrid DFTB3LYP methods with the 6-311+G\*\* basis set through designed isodesmic reactions. The isodesmic reaction processes, that is, the number of each kind of formal bond is conserved, were used with the application of the bond separation reaction (BSR) rules. The molecule was broken down into a set of two heavy-atom molecules containing the same component bonds. The isodesmic reactions used to derive the HOF shown in Scheme S2.



**Scheme S2.** The isodesmic reactions for calculating heat of formation for **2**, **4** and **6**.

The change of enthalpy for the reactions at 298K can be expressed by Equation (1):

$$\Delta H_{298} = \sum \Delta_f H_P - \sum \Delta_f H_R \quad (1)$$

Where  $\sum \Delta_f H_P$  and  $\sum \Delta_f H_R$  are the *HOF* of the reactants and products at 298 K, respectively, and  $\Delta H_{298}$  can be calculated from the following expression in Equation (2):

$$\Delta H_{298} = \Delta E_{298} + \Delta(PV) = \Delta E_0 + \Delta ZPE + \Delta H_T + \Delta nRT \quad (2)$$

where  $\Delta E_0$  is the change in total energy between the products and the reactants at 0 K;  $\Delta ZPE$  is the difference between the zero-point energies (ZPE) of the products and the reactants at 0 K;  $\Delta H_T$  is the thermal correction from 0 to 298 K. The  $\Delta(PV)$  value in Equation (2) is the *PV* work term. It equals  $\Delta nRT$  for the reactions of an ideal gas. For the isodesmic reactions  $\Delta n = 0$ , so  $\Delta(PV) = 0$ . On the left side of Equation (2), apart from target compound all the others are called reference compounds. The HOF of reference compounds are available either from experiments or from the high-level computing such as CBS-4M.

**Table S1.** The optimized Cartesian coordinates for compound **2**.

Atoms	x	y	z
O	5.6963	3.1383	3.9925
N	5.1486	3.8799	4.8123
O	4.6047	4.9203	4.5119



C	5.206	3.4662	6.1971
N	4.7206	4.3725	7.0357
C	5.7459	2.2031	6.5521
N	4.7214	4.1837	8.3391
N	5.7287	2.0582	7.9119
N	6.2111	1.2265	5.8095
C	5.2499	3.016	8.7693
N	6.1373	0.9672	8.6026
H	6.5074	0.4892	6.1895
H	6.2279	1.3081	4.9341
N	5.3611	2.5908	10.0188
C	5.8898	1.3505	9.8622
C	6.0482	0.3821	10.9514
C	5.577	-0.9033	10.8891
C	6.5682	0.4621	12.2535
N	5.8166	-1.4725	12.0785
H	5.1595	-1.3145	10.1427
N	6.4293	-0.6611	12.948
N	7.344	1.5222	12.8303
H	5.6701	-2.2787	12.3031
O	7.5449	2.5143	12.1415
O	7.7942	1.3735	13.967

**Table S2.** The optimized Cartesian coordinates for compound **4**.

Atoms	x	y	z
O	7.0618	4.9793	10.7639
N	6.4277	5.5486	9.893
O	5.7669	4.9885	9.0143
C	6.4194	6.9977	9.9239
N	5.6137	7.6323	9.0904
C	7.0941	7.8785	10.7489
N	5.8	8.8882	9.4312
N	6.6658	9.0994	10.4087
C	8.132	7.7833	11.7742
H	5.4166	9.6059	9.0276
N	8.9286	6.7242	11.882
N	8.3718	8.8206	12.6343
N	9.7463	7.1296	12.8937
C	9.4057	8.4008	13.3247
C	10.7854	6.3983	13.4076
N	10.0932	9.0345	14.3003
N	11.0155	5.2111	12.935
C	11.439	7.1543	14.4103
N	11.1092	8.3872	14.8074
H	10.5075	4.8867	12.2927
H	11.6799	4.7318	13.2544
N	12.5747	6.6114	15.0837
O	12.8959	5.4348	14.8284
O	13.1863	7.2973	15.8997

**Table S3.** The optimized Cartesian coordinates for compound **6**.

Atoms	x	y	z
O	13.1647	2.5981	6.4634
N	12.1659	1.7795	5.9946
N	12.6767	3.4728	7.4558
C	11.0917	2.1229	6.6497
C	11.4014	3.1816	7.5703
C	9.8067	1.4746	6.4185
N	10.5606	3.8287	8.4128
N	8.7484	1.8787	7.1251
N	9.6056	0.4682	5.5354
H	9.8981	3.2887	8.6366
H	11.0002	4.0654	9.1408
N	7.7882	1.0409	6.6434
C	8.3222	0.2041	5.6875
C	6.4954	0.9958	7.0652
N	7.5753	-0.7531	5.0666
N	6.1069	1.8156	8.0105
C	5.7998	-0.0155	6.3662
N	6.3178	-0.8251	5.4317
H	6.6823	2.3829	8.3616
H	5.2748	1.7989	8.2942
N	4.4185	-0.2938	6.6735
O	3.8939	0.3725	7.5834
O	3.8259	-1.1706	6.074

For the gas phase species, heat of formation were calculated as followed:

$$\Delta H_{\text{sub}} = aA^2 + b\sqrt{v\sigma_{\text{tot}}^2} + c$$

$$\Delta H_{\text{f}} (\text{s}) = \Delta H_{\text{f}} (\text{g}) - \Delta H_{\text{sub}}$$

**Table S4.** Calculated total energy ( $E_0$ ), zero-point energy (ZPE), thermal correction to enthalpy ( $H_T$ ) and Solid-Phase heats of formation (HOF).

Compound	$E_0 / \text{a. u.}$	ZPE / $\text{kJ mol}^{-1}$	$\Delta H_T / \text{kJ mol}^{-1}$	HOF(s)/ $\text{kJ mol}^{-1}$
<b>2</b>	-956.1235	312.245662	35.023456	695.0
<b>4</b>	-1133.576477	357.661153	42.186534	821.0
<b>6</b>	-1004.254374	360.7437	39.1383285	710.5
CH <sub>4</sub>	-40.5339263	112.26	10.04	-74.60
1,2,5-oxadiazole	262.183629	114.62	11.84	215.72
1,2,3-triazole	242.3001706	150.23	12.05	233.71
<b>a</b>	428.0233407	221.57	16.25	487.1305385
CH <sub>3</sub> NO <sub>2</sub>	245.0915559	124.93	11.60	-80.80
CH <sub>3</sub> CH <sub>3</sub>	-79.8565413	187.31	11.79	-84.01
CH <sub>3</sub> NH <sub>2</sub>	-95.8938402	160.78	11.64	-22.5

**Table S5.** The heats of formation for heats of Phase change, Gas- and Solid-Phase of compounds **2**, **4** and **6**.

Compound	$\Delta H_{\text{sub}} / \text{kJ mol}^{-1}$	$\Delta H(\text{g}) / \text{kJ mol}^{-1}$	$\Delta H(\text{s}) / \text{kJ mol}^{-1}$
<b>2</b>	147.7	842.7	695.0
<b>4</b>	147.7	968.7	821.0
<b>6</b>	131.4	857.7	710.5

## 6. Crystallographic Data for 2 and 4

Table S6. Crystallographic data for 2, 4 and 6.

	<b>2</b>	<b>4</b>	<b>6</b>
CCDC number	2254742	2190890	2190888
Empirical formula	$\text{C}_7\text{H}_4\text{N}_{10}\text{O}_4$	$\text{C}_6\text{H}_7\text{N}_{11}\text{O}_6$	$\text{C}_9\text{H}_{11}\text{N}_{11}\text{O}_4$
Formula weight	292.2	329.23	337.29
Temperature/K	193	170	170
Crystal system	orthorhombic	monoclinic	monoclinic
Space group	<i>Pbcn</i>	<i>P21/n</i>	<i>C2/c</i>
<i>a</i> /Å	15.467(3)	9.966(2)	34.451(7)
<i>b</i> /Å	6.7622(7)	13.360(3)	4.6905(10)
<i>c</i> /Å	20.528(2)	18.602(4)	20.015(4)
$\alpha$ /°	90	90	90
$\beta$ /°	90	94.827(7)	118.803(6)
$\gamma$ /°	90	90	90
Volume/Å <sup>3</sup>	2147.0(5)	2467.9(9)	2834.2(10)
Z	8	8	8
$\rho_{\text{calc}}/\text{cm}^3$	1.808	1.772	1.581
$\mu/\text{mm}^{-1}$	1.333	0.157	0.129
F(000)	1184	1344	1392
Crystal size/mm <sup>3</sup>	0.13 × 0.11 × 0.1	0.11 × 0.03 × 0.02	0.15 × 0.08 × 0.05
Radiation	CuK $\alpha$ ( $\lambda =$ 1.54178)	MoK $\alpha$ ( $\lambda =$ 0.71073)	MoK $\alpha$ ( $\lambda =$ 0.71073)
2 $\theta$ range for data collection/°	8.614 to 136.772	4.394 to 50.762	4.644 to 52.886
Index ranges	-12 ≤ <i>h</i> ≤ 18, -8 ≤ <i>k</i> ≤ 8, -24 ≤ <i>l</i> ≤ 20	-11 ≤ <i>h</i> ≤ 11, - 16 ≤ <i>k</i> ≤ 15, -22 ≤ <i>l</i> ≤ 22	-42 ≤ <i>h</i> ≤ 42, -5 ≤ <i>k</i> ≤ 5, - 24 ≤ <i>l</i> ≤ 24
Reflections collected	8252	19352	13132
Independent reflections	1956 [R <sub>int</sub> = 0.0511, R <sub>sigma</sub> = 0.0471]	4448 [R <sub>int</sub> = 0.0951, R <sub>sigma</sub> = 0.0877]	2866 [R <sub>int</sub> = 0.0702, R <sub>sigma</sub> = 0.0556]
Data/restraints/parameters	1956/0/195	4448/0/435	2866/0/220
Goodness -of -fit on F <sup>2</sup>	1.033	1.009	1.046

Final R indexes [ $I \geq 2\sigma(I)$ ]	R1 = 0.0460, wR2 = 0.1166	R1 = 0.0601, wR2 = 0.1241	R <sub>1</sub> = 0.0567, wR <sub>2</sub> = 0.1238
Final R indexes [all data]	R1 = 0.0578, wR2 = 0.1266	R1 = 0.1306, wR2 = 0.1609	R <sub>1</sub> = 0.0974, wR <sub>2</sub> = 0.1467
Largest diff. peak/hole / e Å <sup>-3</sup>	0.30/-0.31	0.29/-0.35	0.35/-0.41

**Table S7.** Bond distances in compound **2**.

Parameter	Å	Parameter	Å
O1-N1	1.234(2)	N7-C4	1.357(3)
O2-N1	1.211(2)	N8-N9	1.338(3)
O3-N10	1.224(2)	N8-C6	1.339(3)
O4-N10	1.231(2)	N9-C7	1.328(3)
N1-C1	1.446(3)	N10-C7	1.434(3)
N2-N3	1.318(2)	C1-C2	1.419(3)
N2-C1	1.326(2)	C4-C5	1.467(3)
N3-C3	1.352(3)	C5-C6	1.370(3)

**Table S8.** Bond angles in compound **2**.

Parameter	Bond angle (°)	Parameter	Bond angle (°)
O1-N1-O2	123.40(18)	N3-C3-N4	122.71(18)
O1-N1-C1	116.50(15)	N3-C3-N7	127.64(18)
O2-N1-C1	120.08(17)	N4-C3-N7	109.63(17)
N3-N2-C1	121.84(15)	N6-C4-N7	116.26(17)
N2-N3-C3	116.03(15)	N6-C4-C5	119.32(17)
N6-N4-C2	125.99(15)	N7-C4-C5	124.01(18)
N6-N4-C3	110.48(16)	C4-C5-C6	123.27(18)
C2-N4-C3	123.51(16)	C4-C5-C7	133.76(19)
N4-N6-C4	101.09(15)	C6-C5-C7	102.85(17)
O1-N1-O2	123.40(18)	N3-C3-N4	122.71(18)

**Table S9.** Hydrogen bonds in compound **2**.

D-H...A	d(D-H)/ Å	d(H...A)/ Å	d(D...A)/ Å	<(DHA)/ °
N5-H5A...N6	0.88	2.49	2.805(2)	102
N5-H5A...O4	0.88	2.23	3.076(2)	161
N5-H5B...O1	0.88	2.13	2.688(2)	121
N5-H5B...N9	0.88	2.35	3.185(2)	158

N8-H8...O1	0.85(3)	2.14(3)	2.745(2)	129(2)
C6-H6...N3	0.95	2.24	3.169(3)	164
N5-H5A...N6	0.88	2.49	2.805(2)	102
N5-H5A...O4	0.88	2.23	3.076(2)	161

**Table S10.** Bond distances in compound **4**.

Parameter	Å	Parameter	Å
O1-N1	1.229(5)	N10-C6	1.322(5)
O2-N1	1.246(5)	N11-C6	1.450(6)
O4-N11	1.218(5)	N6-H6B	0.88
O5-N11	1.235(5)	N6-H6A	0.88
O6-N12	1.225(5)	N9-H9	0.91(4)
O7-N12	1.222(5)	O10-H10B	0.87
O11-N21	1.239(5)	O10-H10A	0.87
O12-N21	1.222(5)	N12-C7	1.447(6)

**Table S11.** Bond angles in compound **4**.

Parameter	Bond angle (°)	Parameter	Bond angle (°)
O1-N1-O2	122.3(3)	C9-N17-C10	102.3(3)
O1-N1-C1	119.8(4)	N16-N18-C11	125.0(3)
N3-N2-C1	122.3(3)	C10-N18-C11	124.0(3)
N2-N3-C3	116.3(4)	N16-N18-C10	111.0(3)
C2-N4-C3	124.0(3)	O11-N21-C12	116.5(4)
N4-N5-C4	100.5(3)	O11-N21-O12	116.5(4)
C3-N7-C4	103.1(3)	O12-N21-C12	123.1(4)
N9-N8-C5	104.6(4)	N13-N14-H14	120.3(4)

**Table S12.** Hydrogen bonds in compound **4**.

D-H...A	d(D-H)/ Å	d(H...A)/ Å	d(D...A)/ Å	<(DHA)/ °
O3-H3A...N15	0.87	2.01	2.863(5)	168
O3-H3B...O11	0.87	2.02	2.875(4)	169
N6-H6A...O8	0.88	1.9	2.712(5)	153
N6-H6A...N5	0.88	2.46	2.784(5)	103
N6-H6B...O2	0.88	2.11	2.679(4)	122
N6-H6B...N3	0.88	2.52	3.259(5)	142

**Table S13.** Bond distances in compound **6**.

Parameter	Å	Parameter	Å
O1-N1	1.244(4)	N10-C5	1.304(4)

Parameter	Å	Parameter	Å
O2-N1	1.216(4)	N2-H2B	0.88
O4-N9	1.410(3)	N2-H2A	0.88
O4-N10	1.374(4)	N8-H8A	0.88
O3-C9	1.236(4)	N8-H8B	0.88
N1-C1	1.443(4)	N11-C7	1.448(7)
N2-C2	1.309(4)	N11-C8	1.439(5)
N3-N4	1.311(4)	N11-C9	1.307(4)

**Table S14.** Bond angles in compound **6**.

Parameter	Bond angle (°)	Parameter	Bond angle (°)
N9-O4-N10	111.0(2)	N4-C3-N5	122.0(3)
O1-N1-O2	122.8(3)	N5-C3-N7	109.6(2)
O1-N1-C1	117.2(3)	N4-C3-N7	128.4(3)
O2-N1-C1	120.0(3)	N6-C4-N7	117.0(3)
N4-N3-C1	122.1(2)	N7-C4-C5	124.4(3)
N3-N4-C3	115.9(2)	N6-C4-C5	118.7(2)
N6-N5-C2	125.5(2)	N10-C5-C6	109.8(3)
N6-N5-C3	110.3(2)	C4-C5-C6	128.3(3)

**Table S15.** Hydrogen bonds in compound **6**.

D-H...A	d(D-H)/ Å	d(H...A)/ Å	d(D...A)/ Å	<(DHA)/ °
N2-H2A...O3	0.88	1.89	2.756(3)	168
N2-H2A...N6	0.88	2.46	2.786(4)	102
N2-H2B...O1	0.88	2.11	2.677(4)	122
N2-H2B...O1	0.88	2.3	3.108(4)	152
N8-H8A...O3	0.88	2.44	3.101(4)	132
N8-H8A...N6	0.88	2.37	2.957(4)	125
N8-H8B...N9	0.88	2.36	3.095(4)	141

## 7. Spectrums of Compounds **2**, **4** and **6**.

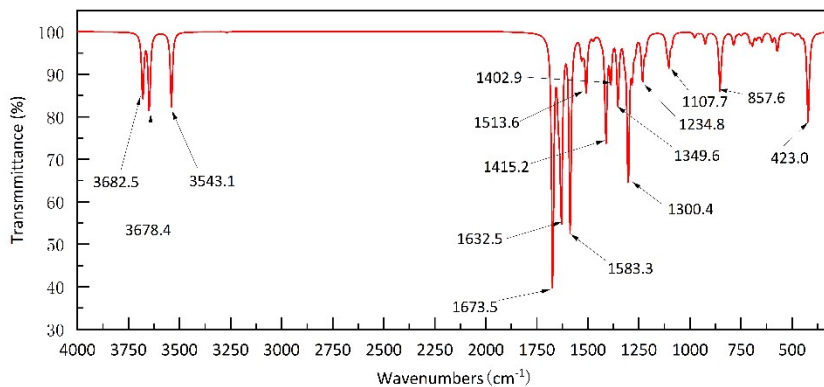


**Figure S4.** The Infrared Spectroscopy Plots for compounds 2.

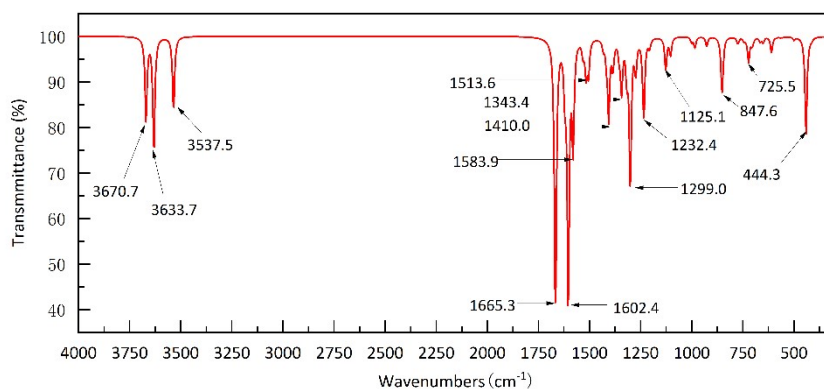


**Figure S5.** The Infrared Spectroscopy Plots for compounds 4.

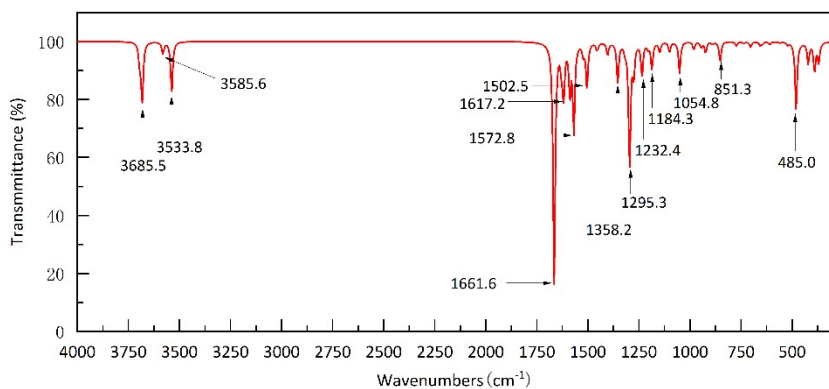


**Figure S6.** The Infrared Spectroscopy Plots for compounds 6.

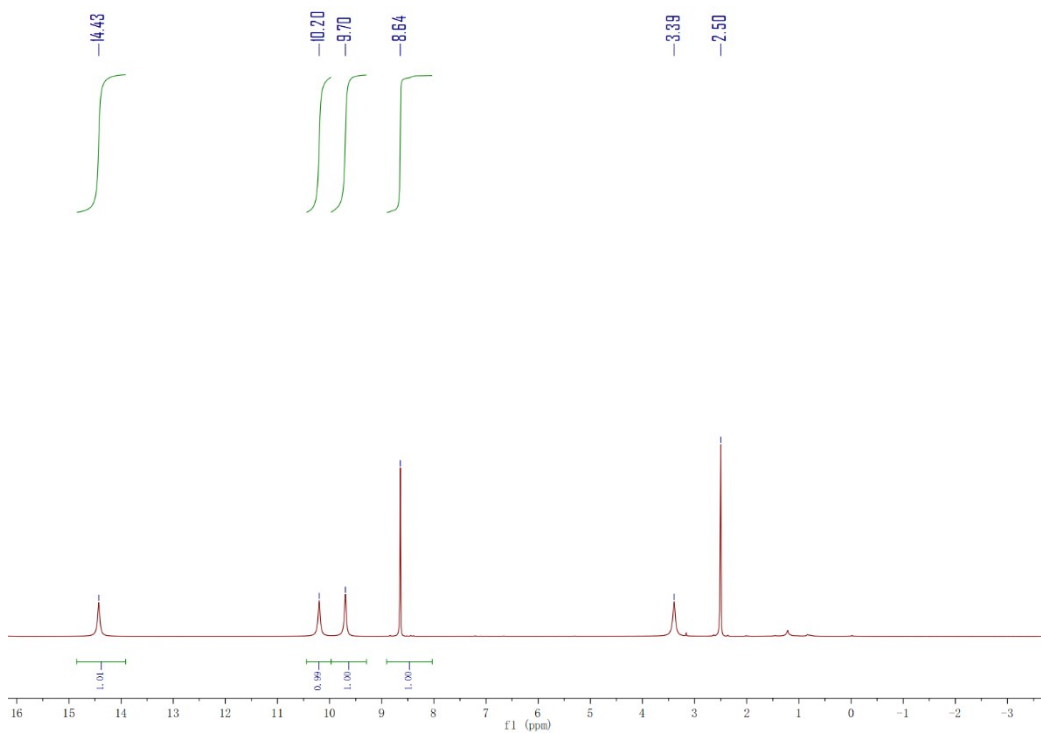


**Figure S7.** <sup>1</sup>H NMR spectra in DMSO-d<sub>6</sub> for compound **2**.

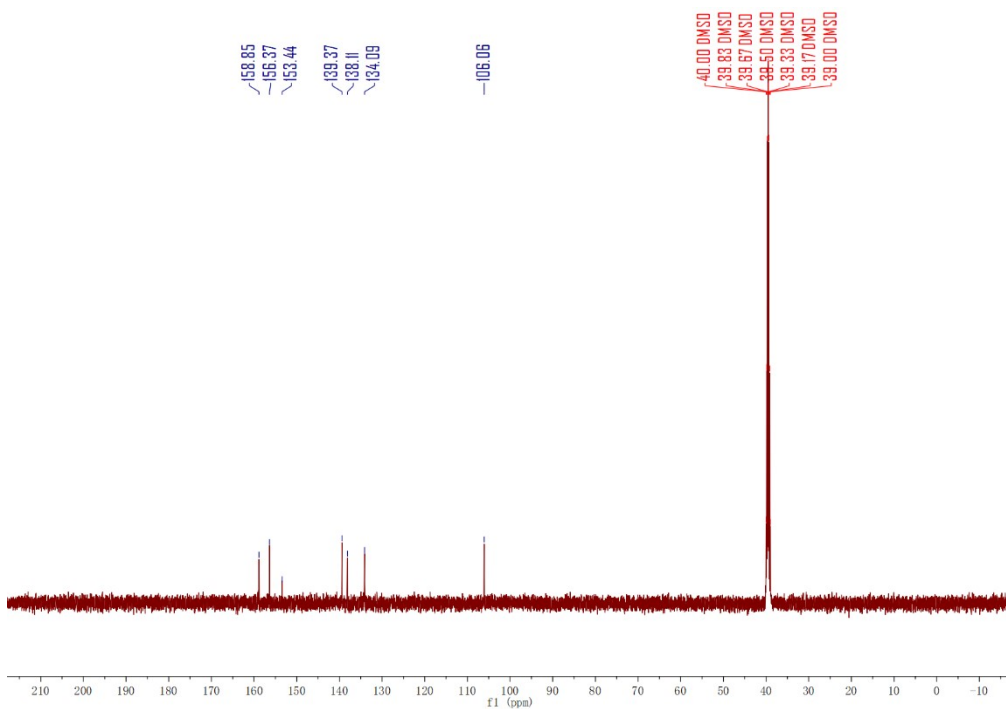


**Figure S8.** <sup>13</sup>C NMR spectra in DMSO-d<sub>6</sub> for compound **2**.



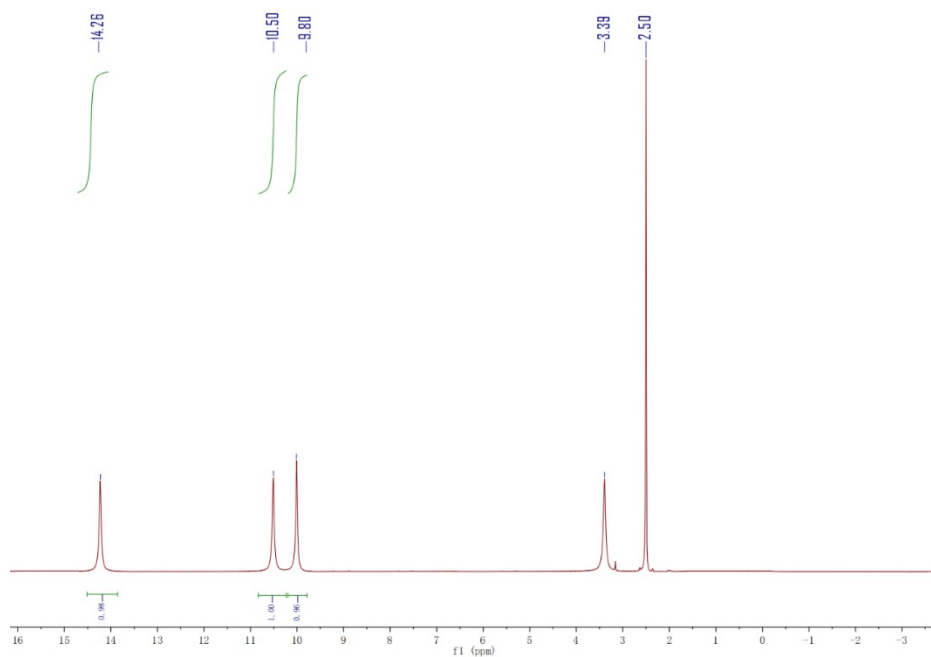


**Figure S9.**  $^1\text{H}$  NMR spectra in  $\text{DMSO-d}_6$  for compound **4**.

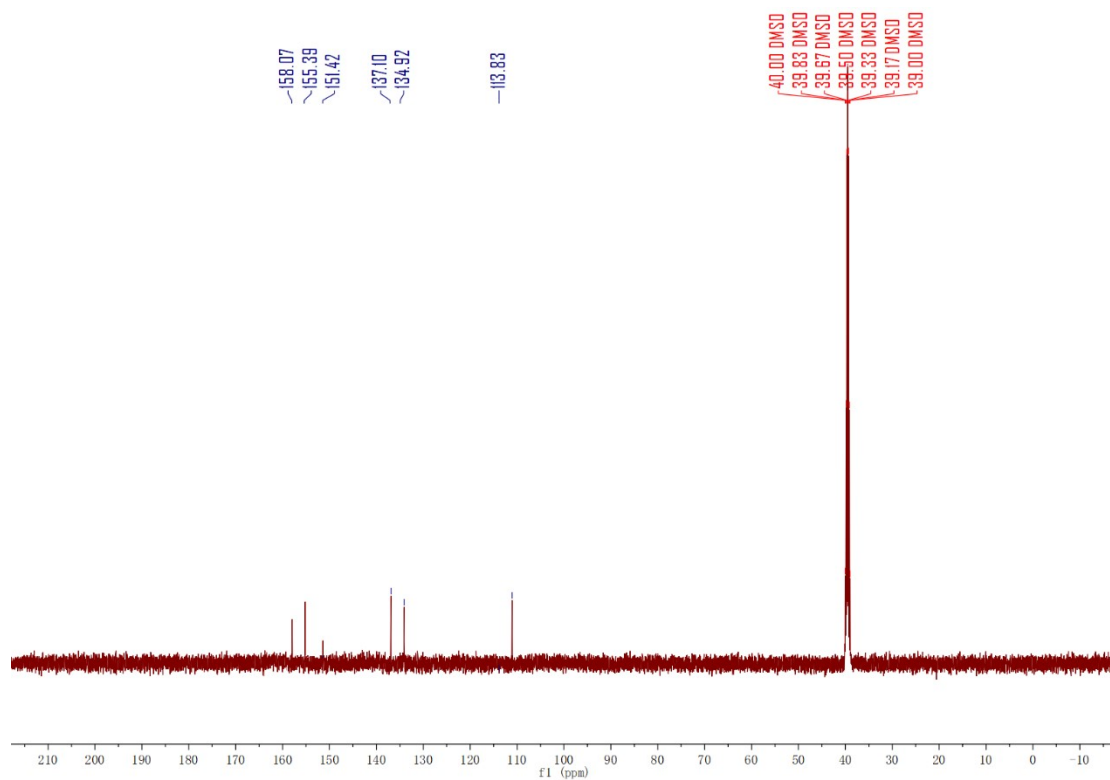


**Figure S10.**  $^{13}\text{C}$  NMR spectra in  $\text{DMSO-d}_6$  for compound **4**.

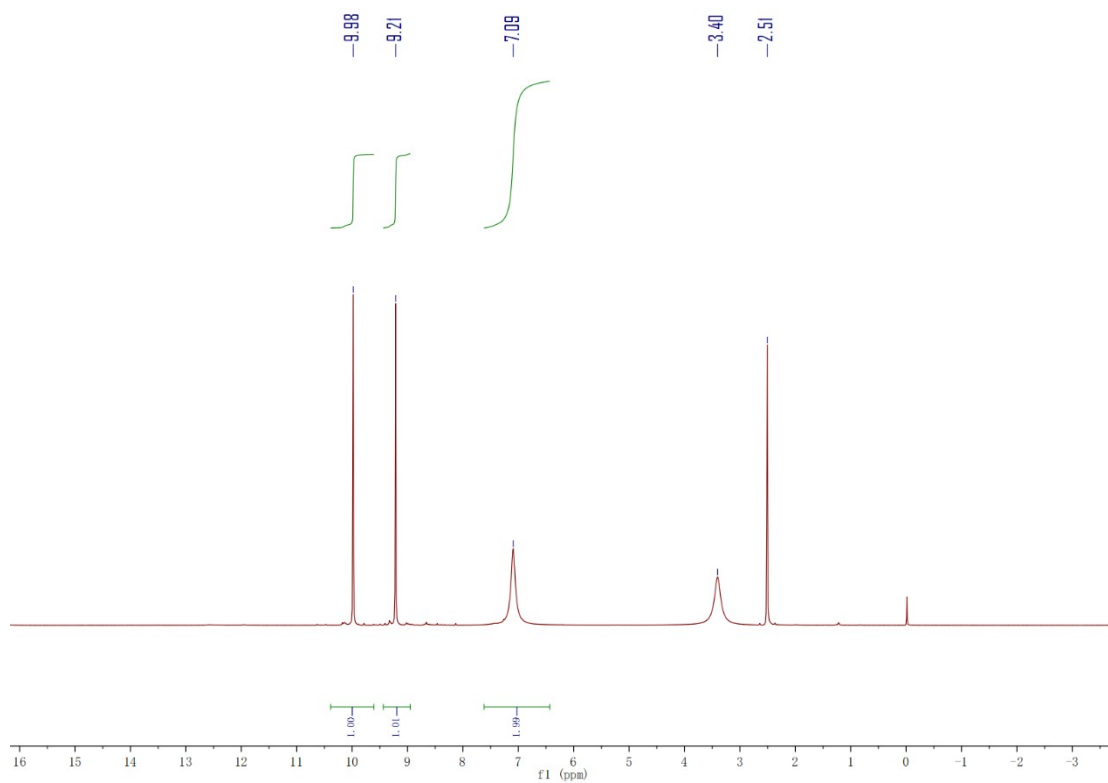


**Figure S11.**  $^1\text{H}$ NMR spectra in  $\text{DMSO-d}_6$  for compound **6**.

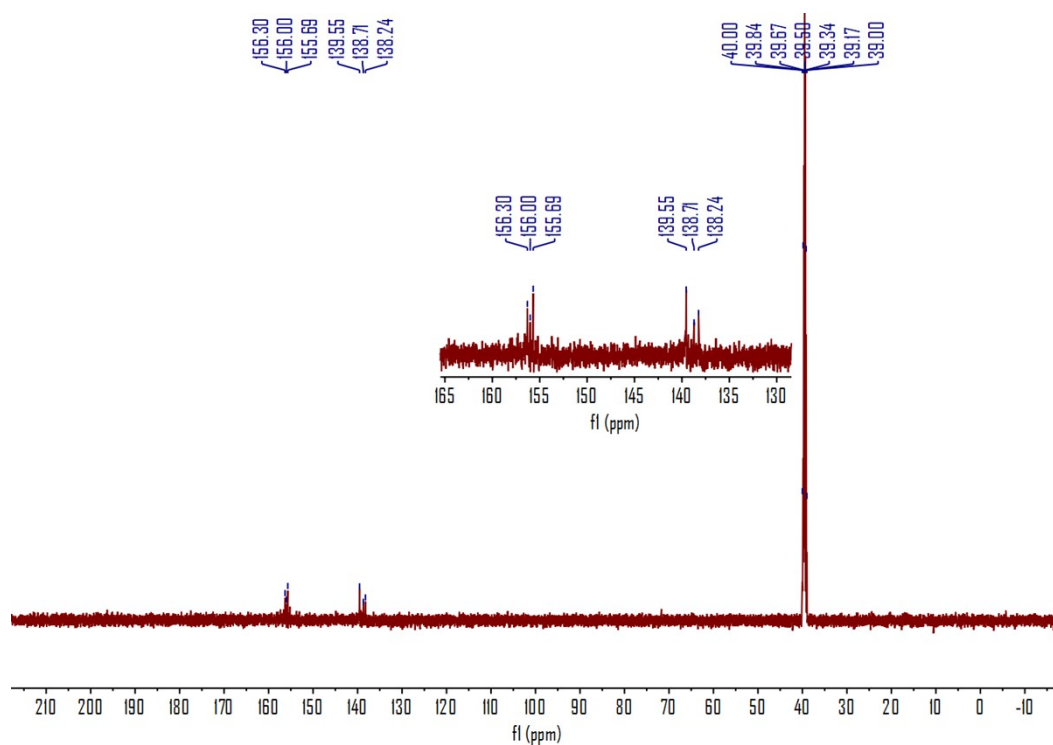


**Figure S12.**  $^{13}\text{C}$  NMR spectra in  $\text{DMSO-d}_6$  for compound **6**.

## 8. References

- [1] M.J.Frisch.Gaussian09,RevisionD.01(GaussianInc.,2009).
- [2] A.D.Becke,J.Chem.Phys.1993,98,5648-5652
- [3] P.J.Stephens;F.J.Devlin;C.F.Chabalowski;M.J.Frisch.J.Phys.Chem.1994,98, 11623-11627.
- [4] P.C.Hariharan;J.A.Pople,Theor.Chim.Acta.1973,28,213-222.
- [5] J.W.Ochterski;G.A.Petersson;J.A.Montgomery,J.Chem.Phys.1996,104,2598-2619.